Heliyon 9 (2023) e16039

Contents lists available at ScienceDirect

Heliyon

journal homepage: www.cell.com/heliyon

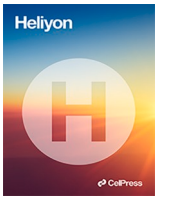

Research article

Twin thickness-dependent tensile deformation mechanism on strengthening-softening of Si nanowires

Mohammed Meaza Yimer, Debela Abeyot Wubeshet, Xiangge Qin *

School of Materials Science and Engineering, Jiamusi University, 258th Xuefu Street, Xiangyang District, Heilongjiang, 154007 PR China

ARTICLE INFO

Keywords:
Silicon nanowire
Twin thickness
Molecular dynamic simulation
Strengthening-softening

ABSTRACT

Twin thickness-dependent deformation and the transition from strengthening to softening in twinned silicon nanowires are investigated using molecular dynamics simulations with cylindrical and hexagonal cross sections. The results show that the transition from strengthening to softening occurs at critical twin thicknesses of 8.1 nm (11.0 TB s) with cylindrical cross section and 11.0 nm (8 TBs) with hexagonal cross section with decreasing twin thickness, and that the strongest twin thickness originates from a transition in the initial plasticity mechanism from full dislocation nucleation and interaction with the TBs to partial dislocation nucleation and gliding parallel to the TBs. Moreover, it is found that the relationship between peak stress and twin thickness can be divided into two regions. Several full and partial dislocations are formed in the regions with strengthening twin thickness range. The accumulation and pile-up of these dislocations and their interaction with the TBs at high density cause the Hall-Petch strengthening behavior. In contrast, few full and partial dislocations are formed with softening twin thickness range. These dislocations are nucleated and propagate parallel to the TBs, resulting in TB migration that causes inverse Hall-Petch softening behavior. Our simulation results provide sufficient insight into the mechanical behavior of twinned silicon nanowires with cylindrical and hexagonal cross sections. The study will be helpful to the further understanding of CTB-related mechanical behaviors of non-metallic materials and non-metallic system.

1. Introduction

One-dimensional semiconductor nanostructure materials consist of nanotubes, nanobelts, and nanowires. Silicon nanowire is also a one-dimensional semiconductor nanowire (NW). Si NWs have attracted a high level of interest due to their unusual and unique behaviors such as mechanical [1,2] and electrical [3], which allow them to be used in a variety of technological advantages such as micro-electromechanical systems (MEMS) and nano-electromechanical systems (NEMS) [4,5]. Nanotwinned structures have been frequently used in engineering materials to improve their mechanical characteristics [6,7]. Previous experiments have shown that, with decreasing twin thickness, the yield strength of nt-Cu increases, reaches a maximum at critical twin thickness of 15 nm, followed by softening with decreasing twin thickness at lower critical values [8,9]. In fact, this strengthening-softening transition phenomena has a great advantage not only to understand the yield strength and plastic deformation behavior of nanotwinned structures, but also to design new nanotwinned materials withimprovedperformance [10–15].

Twin boundaries (TBs) play a significant role in determining both Hall-Petch strengthening and Inverse Hall-Petch softening

* Corresponding author.
E-mail address: qinxiangge@jmsu.edu.cn (X. Qin).

https://doi.org/10.1016/j.heliyon.2023.e16039
Received 21 December 2022; Received in revised form 28 April 2023; Accepted 3 May 2023
Available online 5 May 2023

behavior in twinned NWs [16–20]. The nucleation of dislocation and pile-up formation near to TBs attributed in governing the Hall-Petch strengthening effect, while the interaction of TBs and dislocations contributed in governing an Inverse Hall-Petch softening effect [21–27]. Recently with the remarkable computer simulation development techniques called Molecular Dynamics Method (MD) was developed as an excellent device to perform various researches at nanoscale level. These techniques have been applied to investigate twin thickness dependent yield strength of nanotwinned materials attributable to the strengthening-softening effect under indentation, compression and tension. Based on important knowledge offered by molecular dynamic simulations, the yield strength of twinned copper and magnesium increases with decreasing TBS, below the critical value, the smaller TBS lead to softening mechanism. The accumulation and pile-up of dislocations close to the twin boundary (TB) and the interaction between TBs and dislocation cause enhancement in strength, while the emission and migration of partial dislocations parallel to TBs govern the softening behavior [28–31].

Most of the current investigations of dislocation nucleation and their interaction with TBs, as well as dislocations that glide parallel to TBs, resulting in strengthening-softening transitions, are focused on metallic materials. Although many interesting phenomena regarding the strengthening-softening transition and incipient deformation behavior of non-metallic systems have been uncovered by using MD simulations, the effect of CTBs on the strengthening-softening transition and deformation behavior of non metallic materials is still an open question. Most researches emphasize only the CTBs-induced twin thickness effect as contributing to the strengthening-softening transition, where the nucleation of pile-up dislocations and their interaction with TBs, as well as the gliding of these dislocations parallel to TBs, dominate the deformation mechanisms resulting in Hall-Petch strengthening and Inverse Hall-Petch softening behavior. As a kind of planar defect, it is much easier to understand that CTBs can also show a strengthening-softening effect. Can it be true in non-metallic materials with some twin thickness?

The yield strength-softening behavior of nanograin and nanotwin diamond was investigated by Wen B et al. [32]. The results demonstrate that the compression strength increases with decreasing grain size, maximizing at 153 GPa at d = 8 nm, below which softening takes place. Nobarani H et al. [33] investigated the Hall-Petch and inverse Hall-Petch behaviors on silicon nanopillars using uniform nanotwin (hnt) and gradient nanotwin (gnt) structures under MD simulations. The findings demonstrate that partial dislocation nucleation and migration parallel to TBs promotes the softening behavior, whereas piled-up dislocations and their contact with TBs increase the ultimate strength under tensile and compressive loads. Similarly, the effect of TB spacing [10] is typically attributable to the strengthening-softening phenomenon in metallic NWs [34,35], however a few research only declares that the yield stress increases with decreasing TB spacing, which reveal s strengthening phenomenon [36,37]. Exploring the interaction between TB and dislocations is important to reveal the mechanisms responsible for the enhancement of strength of poly-silicon [38]. Based on experimental research on bi-crystalline silicon, dislocations can be propagate to TB, or pile up on TB [39]. According the recent experimental study, different types of TB are found in silicon, such as Σ3,Σ9 and Σ19 [28], however, Σ3 is the most stable TB and it has

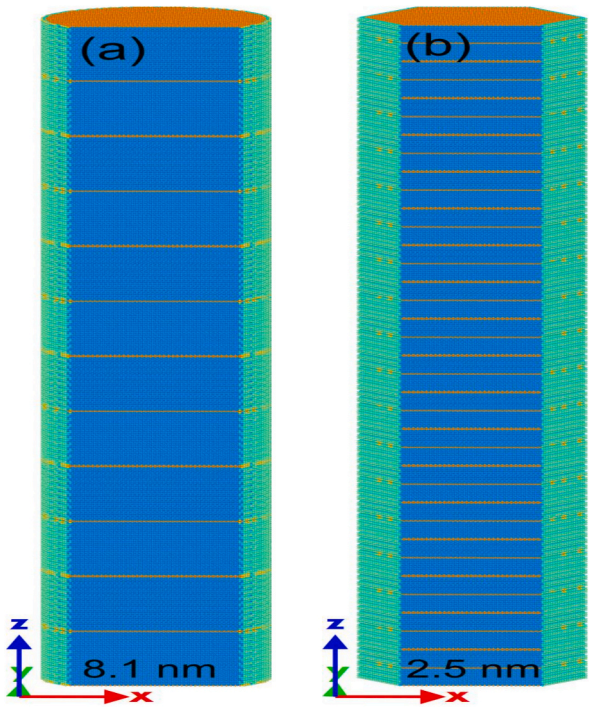

Fig. 1. Atomic configurations of Σ3 TB Si NW, shown in the OVITO software as (a) cylindrical cross section with a twin thickness of 8.1 nm and (b) hexagonal cross section with a twin thickness of 2.5 nm. For each NW, the atoms are colored according to the identify diamond structure (IDS), with blue and green colors representing the cubic diamond structure and brown colors representing the hexagonal diamond structure. (For interpretation of the references to color in this figure, the reader is referred to the web version of this article).

been reported that more than half of the TB in silicon retain the Σ3 structure [40–42]. Among these TB, {111} boundary oriented Σ3 has the lowest surface energy [31,43]. B TB soth experimental and MD simulation show that Σ3 TB exhibits higher resistance to dislocation motion, in the contrary dislocations can penetrate Σ3 TB directly [28,38].

Therefore, a comprehensive understanding of the effect of different twin thickness on the structure and mechanical behaviors of non-metallic materials/systems is far from being completed. In this work, the experimentally observed TBs in silicon of Σ3 type with a plane of {111} is used to generate CTB structure. In order to address the importance of CTB on the mechanical behavior of non-metallic materials/systems, we perform MD simulations of twinned Si NWs with different twin thickness and cross-section under tensile loading. To investigate the mechanical response of Si NWs, the detailed evolution processes of different atomic configurations such as Σ3{111} CTB and dislocations are analyzed. The findings of this study might help in the development of the next generation of semiconductors with improved mechanical performance.

2. Simulation model and method

To investigate the mechanical behavior of Si NWs with Σ3{111} CTBs, we generated seven Σ3 cylindrical cross-section Si NW models in which the model is uniformly divided by 2, 5, 8, 11, 17, 35, and 53 TBs with twin thicknesses of about 33.6 nm, 16.6 nm, 11.0 nm, 8.1 nm, 5.4 nm, 2.5 nm, and 1.6 nm, respectively. In addition, we generated seven hexagonal Σ3 cross-section *Si*-NW models in which the model is uniformly divided by 1, 2, 3, 5, 8, 35, and 53 TBs with twin thicknesses of about 50.7 nm, 33.6 nm, 25.3 nm, 16.6 nm, 11.0 nm, 2.5 nm, and 1.6 nm, respectively. The initial configurations of the twin NWs are constructed by repeating coherent Σ3 twins in the <111>-axis orientation using Atomsk software [44] with a lattice constant of 5.43. <111>-axis oriented NW with cylindrical cross section with eleven TBs (8.1 nm twin thickness) and NW with hexagonal cross section with thirty-five TBs (2.5 nm twin thickness) are shown in Fig. 1(a and b). Due to shortage of time, the quantity of models has been limited. The X, Y, and Z directions of the models are along the <1, −1, 0>, <1, −1, 2>, and <1, −1, −1>, respectively, and Z is the tensile loading direction. The diameter of these NWs is about 20 nm, with a sample length of 101.57 nm. The number of atoms in the cylindrical and hexagonal cross-section computational models is 1,559,304 and 1,297,512, respectively, with an aspect ratio of about 5.0 along the Z axis. All MD simulations are performed using the Large-Scale Atomic Molecular Massively Parallel Simulator (LAMMPS) [45] with the velocity varlet algorithm to integrate the equations of motion in time steps of 2 fs? A reasonable choice of interatomic potential is the basis for the accuracy of molecular dynamics simulation. The Erhart and Albe (EA) [46] potential is one of the most accurate potentials for studying elastic crystal defects, dislocation behavior, plastic deformation, and mechanical properties of silicon [32,47,48]. In the present work, the potential of Erhart and Albe (EA) is used to study the Si–Si atomic interaction and the interaction between dislocations and TB in twinned Si nanowires with CTBs. Periodic boundary conditions were applied along the NW axis, while the NW surfaces were set as stress-free. Before tensile loading, each of the models is equilibrated for 10 ps at 300 K and zero pressure (using a constant NPT ensemble). Then, the Si NW is deformed under tensile loading by adjusting the Z coordinate of each atom according to the applied constant strain rate of 1×10^9/s in the canonical ensemble (NVT, constant volume and temperature). The open-source visualization tool OVITO [49] was implemented to visualize MD data and the crystal structure of twinned Si NWs. Identify diamond structure (IDS) [50] is used to identify the microstructure of NWs, which can distinguish the local crystal structure into cubic and hexagonal diamond.

3. Results and discussion

3.1. The effect of twin thickness on the mechanical behavior

One of the main objectives of this work is to investigate the effects of twin thickness on the mechanical behavior of silicon

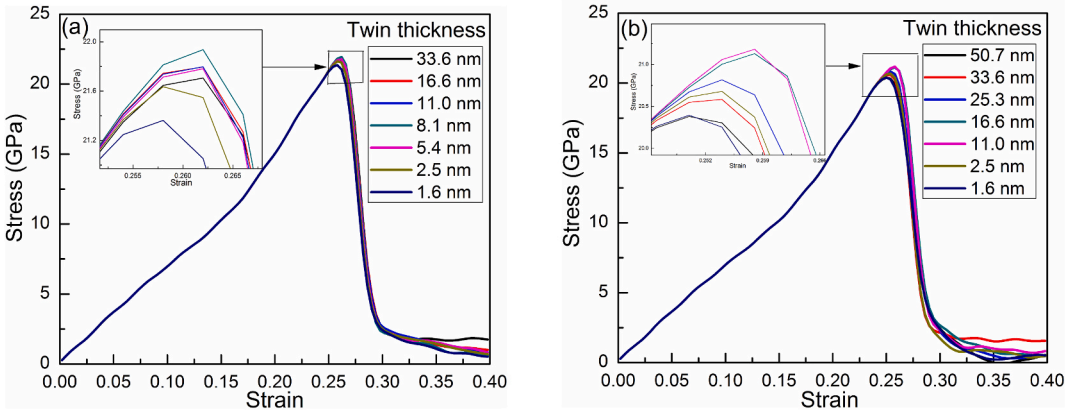

Fig. 2. (a): The tensile stress-strain curves for Si NWs with cylindrical cross-section and twin thicknesses of 33.6 nm, 16.6 nm, 11.0 nm, 8.1 nm, 5.4 nm, 2.5 nm, and 1.6 nm. Fig. 2 (b): The tensile stress-strain curves for hexagonal cross-section Si NWs with twin thicknesses of 50.7 nm, 33.6 nm, 25.3 nm, 16.6 nm, 11.0 nm, 2.5 nm, and 1.6 nm. The enlarged image is the specified region on the stress-strain curve.

nanowires with Σ3{111} CTBs. Uniaxial tensile simulations were applied to the twinned Si nanowires with different twin thicknesses and two different cross sections, i.e., cylindrical and hexagonal cross sections. Fig. 2(a) shows the stress-strain curves for Si NWs with cylindrical cross-section under such conditions with twin thicknesses of 33.6 nm, 16.6 nm, 11.0 nm, 8.1 nm, 5.4 nm, 2.5 nm and 1.6 nm, respectively. Similarly, Fig. 2(b) shows the stress-strain curves for hexagonal cross-section Si NWs with twin thicknesses of 50.7 nm, 33.6 nm, 25.3 nm, 16.6 nm, 11.0 nm, 2.5 nm, and 1.6 nm, respectively. Similarly, Fig. 2(b) shows the stress-strain curves for hexagonal cross-section Si NWs with twin thicknesses of 50.7 nm, 33.6 nm, 25.3 nm, 16.6 nm, 11.0 nm, 2.5 nm, and 1.6 nm, respectively. As can be seen from Fig. 2(a) and (b), in all cases the tensile stress increases linearly with strain up to a certain peak stress (at this point the stress is defined as the yield strength). The peak stress is related to the onset of plastic deformation, before and after which the stress stages are defined as elastic stage and plastic stage, respectively. For all twinned Si NWs with different twin thicknesses, the results showed that the peak stress gradually increases with decreasing twin thickness, reaching a maximum at 8.1 nm and 11.0 nm for cylindrical and hexagonal NWs, respectively, followed by softening at smaller values. This shows a transition from strengthening to softening as a function of twin thickness, where we reveal the maximum peak stress. The strongest twin thickness is originates from a transition in the initial plasticity mechanism from full dislocation nucleation and interaction with the TBs to partial dislocation nucleation and gliding parallel to the TBs. This strengthening/softening result agrees well with recent experimental and MD simulation results for nanotwinned copper and platinum when the twin thickness is reduced to a critical value [9,15,29–32,35]. It should be noted that our observations are different from the phenomenon of transition from strengthening to softening in Si pillars reported in the previous study by Nobarani H et al. [33]. Moreover, as can be seen Fig. 2(a and b), cylindrical cross-section NWs with 11 TBs, i.e., twin thickness of 8.1 nm, and hexagonal cross-section NWs with 8 TBs, i.e., twin thickness of 11.0 nm, produce the highest strengths of ~21.936 GPa and ~21.182 GPa at the peak stress, respectively. It can be seen that the NW reaches its maximum strength at this point and the critical value of the twin thickness is observed and the variation in the peak stress is around 5% for both cross-sections.

The variation of peak stress as a function of twin thickness is shown in Fig. 3(a and b) for all fourteen Si NWs with cylindrical and hexagonal cross sections. In Fig. 3(a), for Si NWs with cylindrical cross-section, it is clearly seen that the peak stress gradually increases with decreasing twin thickness from 33.6 nm to 8.1 nm, which shows the trend of Hall-Petch relationship; however, the peak stress decreases with decreasing twin thickness from 8.1 nm to 1.6 nm, which shows the trend of inverse Hall-Petch relationship. Moreover, it can be seen in Fig. 3(b) for Si NWs with hexagonal cross-section that the peak stress gradually increases with decreasing twin thickness from 50.7 nm to 11.0 nm, showing a Hall-Petch relationship; however, the peak stress decreases with decreasing twin thickness from 11.0 nm to 1.6 nm, showing an inverse Hall-Petch relationship. Recent experimental findings [9,15,21,35] and simulated results [20, 34] are in qualitative agreement with the Hall-Petch and inverse Hall-Petch relationship phenomena. The results show that during tensile deformation of twinned Si NWs with cylindrical and hexagonal cross sections, the Hall-Petch and inverse Hall-Petch relationships exist as a function of twin thickness. In Section 3.2, the details of tensile deformation in twinned Si NWs are discussed at the atomic level to reveal the underlying mechanisms of such a relationship.

3.2. *The effect of twin thickness on the deformation mechanism*

According to the above analysis, twin thickness affects the mechanical behavior of twinned Si NWs, and this can be divided into a strengthening range (33.6 = nm twin thickness ≥8.1 nm) for NWs with cylindrical cross section and a softening range (twin thickness <8.1 nm) for NWs with hexagonal cross section. This indicates that the deformation mechanisms in the two ranges are not similar. To illustrate the different deformation mechanisms, the different atomic configurations in the twinned Si NWs with twin thicknesses of 11.0 nm and 2.5 nm are discussed under uniaxial processes. These two cases correspond to the two different twin thickness ranges, respectively, which are the same for both cross sections.

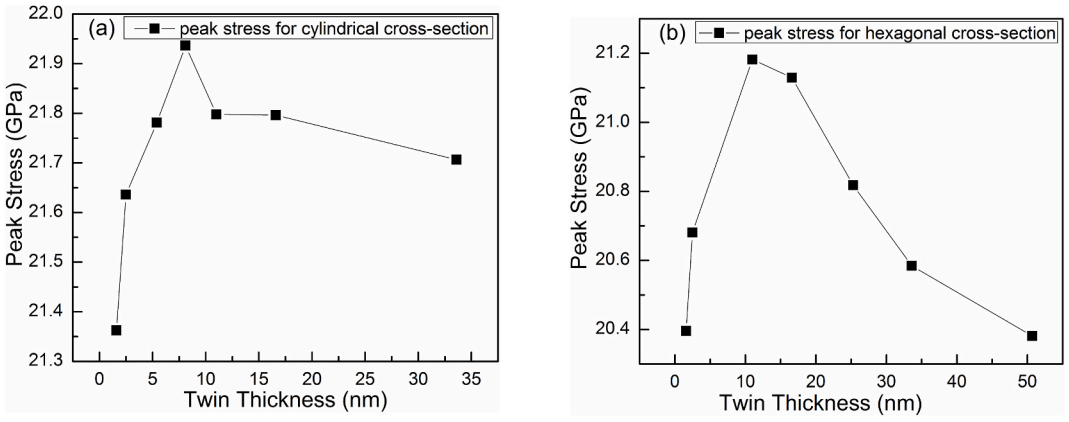

Fig. 3. Peak stress as a function of twin thickness from (a) 33.6 nm–1.6 nm for cylindrical cross-section and from (b) 50.7 nm–1.6 nm for hexagonal cross-section of Si NWs.

3.2.1. Strengthening twin thickness range (33.6 nm ≥ twin thickness ≥8.1 nm) and (50.7 nm ≥ twin thickness ≥11.0 nm)

Fig. 4(b, b') and (a) show the atomic configuration and stress-strain curve of twinned Si NWs with a twin thickness of 11.0 nm (8 CTBs) during the uniaxial tensile process. The specimens were taken at four strain points (A_1-D_1) and (A_2-D_2). For a clear visualization, the atoms of cubic diamond and other types are removed, leaving only hexagonal diamond atoms. In the elastic stage (0 -<A_1,A_2>: 0 < ε < 0.26), as shown in Fig. 4(a), the number of atoms remains unchanged, indicating that the twinned *Si*-NW retains its original configuration.

At the following plastic stage (<B_1,B_2>: 0.26 = ε ≤ 0.30), the stress drops rapidly in the stress-strain curve shown in Fig. 4(a). At this point, several 1/2<110>{111} Full dislocations nucleate between TBs and free surfaces, as shown in Fig. 4(b, b'). With increasing strain (<C_1,C_2>,<D_1,D_2>: 0.33 = ε ≤ 0.36), the leading 1/2<110>{111} Full dislocations propagate and interact with the TBs; pile-ups form, as highlighted by solid squaresin Fig. 4(b, b'); such pile-ups serve as new sources of dislocation nuclei that generate another 1/6<112>{111} Partial dislocations. In fact, the accumulation of dislocations in twinned silicon is related to the twin thickness. As a result, the density of accumulated 1/2<110>{111} Full dislocations and 1/6<112>{111} Partial dislocations decrease relative to TBs with decreasing twin thickness, from 33.6 nm to 8.1 nm for cylindrical cross sections and from 50.7 nm to 11.0 nm for hexagonal cross sections. The interaction of accumulated and piled-up dislocations with TBs at high density is the reason for strengthening of NWs. An experimental study on the piled-up screw dislocation characteristics around GB/TB was observed on multicrystalline silicon [41].

3.2.2. Softening twin thickness range (twin thickness <8.1 nm) and (twin thickness <11.0 nm)

Fig. 4(d, d') and 4(c) show the atomic configuration and stress-strain curve of twinned Si NWs with a twin thickness of 2.5 nm (35 CTBs) during the uniaxial tensile process. The specimens were taken at four strain points (A_1-D_1) and (A_2-D_2). For a clear visualization,

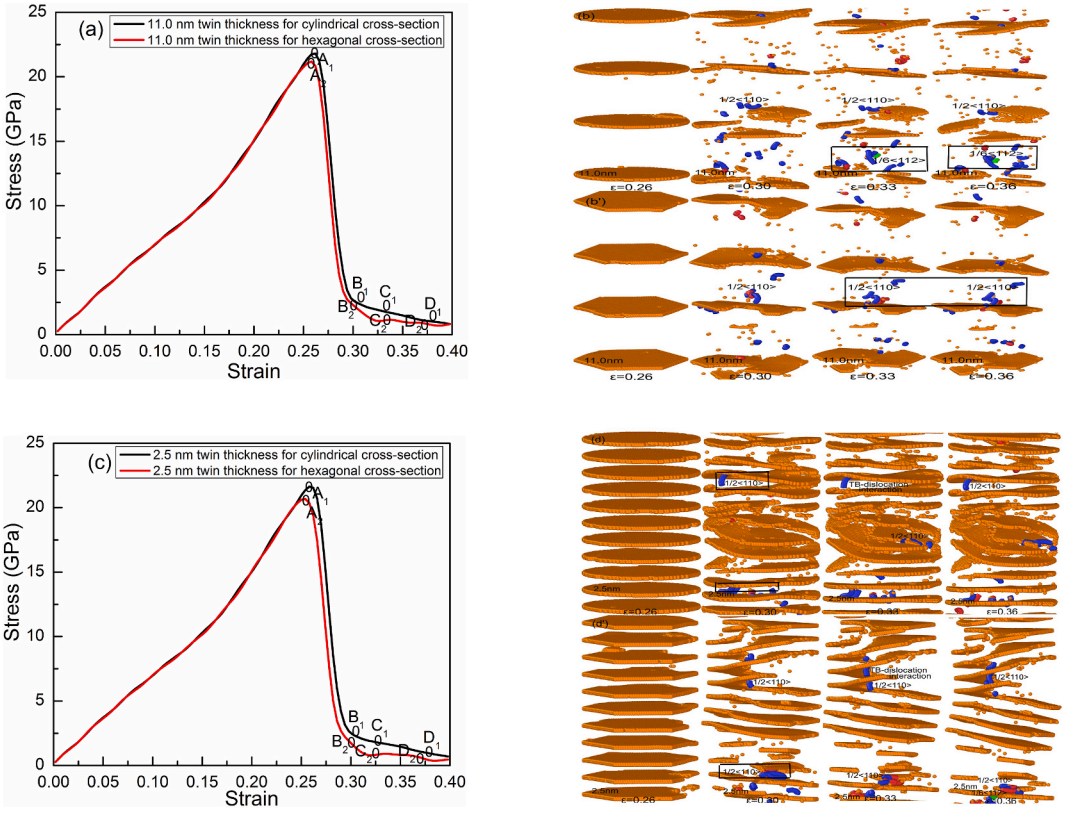

Fig. 4. (a) The stress-strain curves for tensile specimens with twin thickness = 11.0 nm and with (b) cylindrical and (b') hexagonal cross-section at 300 K. (a) And points (A_1-D_1) and (A_2-D_2) are the four strain points of the stress-strain curve for the specimens with twin thickness = 11.0 nm (b, b'), sliced atomic configurations for a sample with cylindrical cross section and twin thickness = 11.0 nm: (a) ε = 0.26 (point A_1), (b) ε = 0.30 (point B_1), (c) ε = 0.33 (point C_1), (d) ε = 0.36 (point D_1), and for a specimen with hexagonal cross section and twin thickness = 11.0 nm: (a) ε = 0.26 (point A_2), (b) ε = 0.30 (point B_2), (c) ε = 0.33 (point C_2), (d) ε = 0.36 (point D_2). The atoms are colored according to the IDS. (For interpretation of the references to color in this figure, the reader is referred to the web version of this article). (c) The stress-strain curves for tensile specimens with twin thickness = 2.5 nm and with (d) cylindrical and (d') hexagonal cross section at 300 K (c) and points (A_1-D_1) and (A_2-D_2) are the four strain points of the stress-strain curve for the specimens with twin thickness = 2.5 nm (d, d'), sliced atomic configurations for a specimen with cylindrical cross section and twin thickness = 2.5 nm: (a) ε = 0.26 (point A_1), (b) ε = 0.30 (point B_1), (c) ε = 0.33 (point C_1), (d) ε = 0.36 (point D_1), and for a sample with hexagonal cross section and twin thickness = 2.5 nm: (a) ε = 0.26 (point A_2), (b) ε = 0.30 (point B_2), (c) ε = 0.33 (point C_2), (d) ε = 0.36 (point D_2). The atoms are colored according to the IDS. (For interpretation of the references to color in this figure, the reader is referred to the web version of this article.).

the atoms of cubic diamond and other types are removed, leaving only hexagonal diamond atoms. The number of atoms remains unchanged in the elastic stage (0 -<A_1,A_2>: $0 < \varepsilon < 0.26$), as shown in Fig. 4(c), indicating that the twinned *Si*-NW retains its original configuration.

At the following plastic stage (<B_1,B_2>: $0.26 = \varepsilon \leq 0.30$), the stress drops rapidly in the stress-strain curve shown in Fig. 4(c). At this point, some 1/2<110>{111} Full dislocations nucleate and glide parallel to the TBs, as indicatedby solid squaresin Fig. 4(d, d'). With increasing strain (<C_1,C_2>,<D_1,D_2>: $0.33 = \varepsilon \leq 0.36$), the TB migration results from the gliding of some 1/2<110>{111} Full dislocations and 1/6<112> partial dislocations parallel to the TBs that dominate the deformation mechanism. These dislocations rarely encountered obstacles until they reached the other side of the TBs and were blocked by them. As a result, the nucleation and movement of some 1/2<110>{111} Full dislocations and 1/6<112>{111} partial dislocations along the TBs as well as the TB migration attributed to the softening behavior of twinned Si NWs with decreasing twin thickness. The interaction of dislocations with TB and TB migration phenomena was also consistent with in situ tensile tests on twinned Pt nanocrystals [51]. Moreover, at the plastic stage (<C_1,C_2>,<D_1,D_2>): $0.33 = \varepsilon \leq 0.36$), the activation of some 1/2<110>{111} Full dislocations and 1/6<112> partial dislocations contribute to the formation of multiple shear bands, and these shear bands lead to the nucleation and propagation of cracks along the TBs before fracture in the twinned Si NWs, as shown in Fig. 5. This phenomenon is consistent with previous experimental results in Si NWs [52,53].

It can be concluded that the inverse Hall-Petch relationship of twinned Si NWs as a function of twin thickness during tensile loading can be attributed to a transition of deformation mechanisms occurring at a critical twin thickness (8.1 nm for a cylindrical cross-section) and twin thickness (11.0 nm for a hexagonal cross-section) for which peak strength is maximized. It is important to keep in mind that the transition of the deformation processes at the critical twin thickness is a progressive process rather than an abrupt change. For NWs with twin thickness ranging from 8.1 nm to 33.6 nm with a cylindrical cross-section and from 11.0 nm to 50.7 nm with a hexagonal cross-section, the nucleation of partial dislocations and their interaction with TBs, as well as the pile-up of those dislocations parallel to the TBs, accommodate the majority of the deformation mechanism, resulting in Hall-Petch strengthening behavior. Similarly, when twin thickness decreases to a value less than 8.1 nm with a cylindrical cross-section and 11.0 nm with a hexagonal cross-section, the nucleation of a few partial dislocations and gliding parallel to the TBs accommodate most of the deformation mechanism, resulting in inverse Hall-Petch softening behavior. Generally, the concentrations of dislocation on free surfaces of NWs above the critical twin thickness are higher than those below the critical twin thickness, which will cause a higher peak strength.

4. Conclusion

The effect of twin thickness on the mechanical behavior of twinned Si nanowires with cylindrical and hexagonal cross-sections is simulated by MD simulations. The details of deformation mechanisms are analyzed in terms of the evolutions of various atomic configurations, such as Σ3{111} CTBs and dislocations. Our findings are summarized as follows.

- The result demonstrates that twin thickness has a mutual effect on the mechanical behavior of twinned Si nanowires. The strengthening-to-softening transition occurs at critical twin thickness of 8.1 nm (8 TBs) with a cylindrical cross-section and 11.0 nm (53 TBs) with a hexagonal cross-section, with decreasing twin thickness. The softening is observed with small twin thickness, and the strengthening is observed with large twin thickness. The strongest twin thickness originates from a transition in the initial plasticity mechanism from full dislocation nucleation and intersecting with the TBs to partial dislocation nucleation and gliding parallel to the TBs.

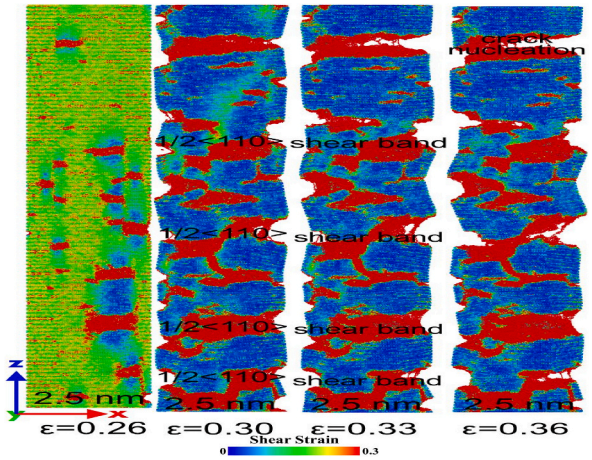

Fig. 5. Shows the formation of a shear band and crack in twinned Si NW with a twin thickness of 2.5 nm (35 TBs) at different strain values (a) $\varepsilon = 0.26$, (b) $\varepsilon = 0.30$, (c) $\varepsilon = 0.33$, (d) $\varepsilon = 0.36$. Atoms are colored according to von Shear strain. (For interpretation of the references to color in this figure, the reader is referred to the web version of this article.).

- The peak stress increases with decreasing twin thickness, reaching its maximum, in which a Hall-Petch relationship is observed, followed by decreases at smaller values, in which an inverse Hall-Petch relationship is reported. However, the critical value at maximum strength significantly depends on twin thickness.
- It is found that TBs in the silicon nanowires can lead to a strengthening or softening effect, and the relationship of peak strength with twin thickness can be divided into two ranges, that is, the strengthening twin thickness range (33.6 nm $\geq$ twin thickness $\geq$8.1 nm) with a cylindrical cross-section as well as (50.7 nm $\geq$ twin thickness $\geq$11.0 nm) with a hexagonal cross-section, and the softening twin thickness range (twin thickness<8.1 nm) and (twin thickness<11.0 nm).
- It is found that TBs in the silicon nanowires can lead to a strengthening or softening effect, and the relationship of peak strength with twin thickness can be divided into two ranges, that is, the strengthening twin thickness range (33.6 nm $\geq$ twin thickness $\geq$8.1 nm) with a cylindrical cross-section as well as (50.7 nm $\geq$ twin thickness $\geq$11.0 nm) with a hexagonal cross-section, and the softening twin thickness range (twin thickness<8.1 nm) and (twin thickness<11.0 nm) with a cylindrical and hexagonal cross-section, respectively.
- The twinned silicon nanowires with various twin thicknesses and cross-sections display different deformation mechanisms during the uniaxial tensile processes. For that, with strengthening twin thickness range (33.6 nm $\geq$ twin thickness $\geq$8.1 nm) and (50.7 nm $\geq$ twin thickness $\geq$11.0 nm), several 1/2<110>{111} full as well as 1/6<112>{111} partial dislocations are formed. The accumulation and pile-up of these dislocations and their interaction with TBs under high density cause strengthening behavior in twinned Si NWs.
- For that with softening twin thickness range (twin thickness <8.1 nm) and (twin thickness <11.0 nm), a few 1/2<110>{111} full and 1/6<112>{111} partial dislocations are formed. The nucleation and propagation of those dislocations, which glide parallel to TBs, results in TB migration, and this phenomenon causes softening behavior in the twinned Si NWs. Furthermore, shear bands form at the top of nanowires. The formation of shear bands is attributed to the nucleation and propagation of cracks along TBs before fracture.

This study demonstrates the effect of twin thickness with Σ3{111} CTB on the mechanical behavior of materials with cylindrical and hexagonal cross-sections in order to design nanotwinned non-metallic materials with sufficient peak stress. The findings of this research might help to develop the synthesis of the next generation of semiconductors with improved mechanical performance.

Author contribution statement

Mohammed Meaza Yimer, Debela Abiyot Wubeshet, Xiangge Qin: Conceived and designed the experiments; Performed the experiments; Analyzed and interpreted the data; Contributed reagents, materials, analysis tools or data; Wrote the paper.

Funding statement

The work is supported the National Natural Science Foundation of China (51271089). We are grateful to Chinese Government Scholarship for International Students.

Data availability statement

Data will be made available on request.

Additional information

No additional information is available for this paper.

Declaration of competing interest

The authors declare that they have no known competing financial interests or personal relationships that could have appeared to influence the work reported in this paper

References

[1] X.D. Han, et al., Low-temperature in situ large-strain plasticity of silicon nanowires, Adv. Mater. 19 (2007).
[2] Y. Cui, et al., Doping and electrical transport in silicon nanowires, J. Phys. Chem. B 104 (2000) 5213–5216.
[3] S. Hoffmann, et al., Measurement of the bending strength of vapor-liquid-solid grown silicon nanowires, Nano Lett. 6 (4) (2006) 622–625.
[4] A.A. Husain, et al., Nanowire-based very-high-frequency electromechanical resonator, Appl. Phys. Lett. 83 (2003) 1240–1242.
[5] M. Liao, et al., Suspended single-crystal diamond nanowires for high-performance nanoelectromechanical switches, Adv. Mater. 22 (2010).
[6] Z. Cheng, et al., Extra strengthening and work hardening in gradient nanotwinned metals, Science (2018) 362.
[7] N. Zhang, M. Asle Zaeem, Effects of twin boundaries and pre-existing defects on mechanical properties and deformation mechanisms of yttria-stabilized tetragonal zirconia, J. Eur. Ceram. Soc. 40 (2020) 108–114.
[8] K. Lu, L. Lu, S.B. Suresh, Strengthening materials by engineering coherent internal boundaries at the nanoscale, Science 324 (2009) 349–352.
[9] L. Lu, et al., Revealing the maximum strength in nanotwinned copper, Science 323 (2009) 607–610.
[10] B. Hyde, H.D. Espinosa, D. Farkas, An atomistic investigation of elastic and plastic properties of Au nanowires, J. Occup. Med. 57 (2005) 62–66.

[11] C. Deng, F. Sansoz, Size-dependent yield stress in twinned gold nanowires mediated by site-specific surface dislocation emission, Appl. Phys. Lett. 95 (2009), 091914.
[12] Y. Gao, et al., Twin boundary spacing-dependent deformation behaviours of twinned silver nanowires, Mol. Simulat. 41 (2015) 1546–1552.
[13] X. Guo, Y. Xia, Repulsive force vs. source number: competing mechanisms in the yield of twinned gold nanowires of finite length, Acta Mater. 59 (2011) 2350–2357.
[14] F. Hammami, Y. Kulkarni, Size effects in twinned nanopillars, J. Appl. Phys. 116 (2014), 033512.
[15] L. Wang, et al., In situ atomic-scale observation of grain size and twin thickness effect limit in twin-structural nanocrystalline platinum, Nat. Commun. 11 (2020).
[16] S.K. Zhong, et al., Nanoscale twinned copper nanowire formation by direct electrodeposition, Small 5 20 (2009) 2265–2270.
[17] A. Cao, Y. Wei, S.X. Mao, Deformation mechanisms of face-centered-cubic metal nanowires with twin boundaries, Appl. Phys. Lett. 90 (2007), 151909.
[18] C. Deng, F. Sansoz, Near-ideal strength in gold nanowires achieved through microstructural design, ACS Nano 3 10 (2009) 3001–3008.
[19] K.A. Afanasyev, F. Sansoz, Strengthening in gold nanopillars with nanoscale twins, Nano Lett. 7 (2007) 2056–2062.
[20] J. Wang, et al., Strong Hall-petch type behavior in the elastic strain limit of nanotwinned gold nanowires, Nano Lett. 15 (6) (2015) 3865–3870.
[21] Z. Li, et al., Dynamic mechanisms of strengthening and softening of coherent twin boundary via dislocation pile-up and cross-slip, Mater. Res. Letters 10 (2022) 539–546.
[22] Q. Huang, et al., Nanotwinned diamond with unprecedented hardness and stability, Nature 510 (2014) 250–253.
[23] K. Lu, Stabilizing nanostructures in metals using grain and twin boundary architectures, Nat. Rev. Mater. 1 (2016), 16019.
[24] L.L. Shaw, A.L. Ortiz, J.C. Villegas, Hall–Petch relationship in a nanotwinned nickel alloy, Scripta Mater. 58 (2008) 951–954.
[25] Z.S. You, et al., Plastic anisotropy and associated deformation mechanisms in nanotwinned metals, Acta Mater. 61 (2013) 217–227.
[26] Y. Zhu, X. Liao, X. Wu, Deformation twinning in nanocrystalline materials, Prog. Mater. Sci. 57 (2012) 1–62.
[27] B. Li, H. Sun, C. Chen, Extreme mechanics of probing the ultimate strength of nanotwinned diamond, Phys. Rev. Lett. 117 11 (2016), 116103.
[28] A. Stukowski, K. Albe, D. Farkas, Nanotwinned fcc metals: strengthening versus softening mechanisms, Phys. Rev. B 82 (2010), 224103.
[29] X. Li, et al., Dislocation nucleation governed softening and maximum strength in nano-twinned metals, Nature 464 (2010) 877–880.
[30] J. Xiao, et al., Strengthening-softening Transition in Yield Strength of Nanotwinned Cu. Scripta Materialia, 2019.
[31] H.Y. Song, Y. Li, Effect of twin boundary spacing on deformation behavior of nanotwinned magnesium, Phys. Lett. 376 (2012) 529–533.
[32] B. Wen, et al., Continuous strengthening in nanotwinned diamond, npj Comput. Mater. 5 (2019) 1–6.
[33] H. Nobarani, et al., Nanotwin-induced strengthening in silicon: a molecular dynamics study, Int. J. Mech. Sci. 189 (2020), 105990.
[34] H.Y. Song, Y. Sun, Effect of coherent twin boundary and stacking fault on deformation behaviors of copper nanowires, Comput. Mater. Sci. 104 (2015) 46–51.
[35] 魏宇杰, Anisotropic size effect in strength in coherent nanowires with tilted twins, Phys. Rev. B (2011) 84.
[36] L. Hao, et al., Mechanical behavior of metallic nanowires with twin boundaries parallel to loading axis, Comput. Mater. Sci. 169 (2019) 1–9.
[37] Z. Hou, et al., Effect of twin boundary spacing on the deformation behaviour of Au nanowire, Physica B-condensed Matter 581 (2020), 411952.
[38] H. Chen, V.I. Levitas, L. Xiong, Slip of shuffle screw dislocations through tilt grain boundaries in silicon, Comput. Mater. Sci. 157 (2019) 132–135.
[39] M.E. Martínez-Hernández, et al., Dislocations at grain boundaries in deformed silicon, Phil. Mag. 56 (1987) 641–658.
[40] C. Liu, et al., Multiple silicon nanotwins formed on the eutectic silicon particles in Al-Si alloys, Scripta Mater. 64 (2011) 339–342.
[41] I. Yonenaga, K. Kutsukake, Transmission behavior of dislocations against Σ3 twin boundaries in Si, J. Appl. Phys. 127 (2020), 075107.
[42] J. Chen, et al., Carrier recombination activities and structural properties of small-angle boundaries in multicrystalline silicon, Solid State Phenom. 131–133 (2007) 14–19.
[43] Y. Wang, R. Smirani, G.G. Ross, Nanotwinning in silicon nanocrystals produced by ion implantation, Nano Lett. 4 (2004) 2041–2045.
[44] P. Hirel, Atomsk: a tool for manipulating and converting atomic data files, Comput. Phys. Commun. 197 (2015) 212–219.
[45] S.J. Plimpton, Fast parallel algorithms for short-range molecular dynamics, J. Comput. Phys. 117 (1993) 1–19.
[46] P. Erhart, K. Albe, Analytical potential for atomistic simulations of silicon, carbon, and silicon carbide, Phys. Rev. B 71 (2005), 035211.
[47] C. Baruffi, C. Brandl, On the structure of (111) twist grain boundaries in diamond: atomistic simulations with Tersoff-type interatomic potentials, Acta Mater. 215 (2021), 117055.
[48] G. Mogni, et al., Molecular dynamics simulations of shock-compressed single-crystal silicon, Phys. Rev. B 89 (2014).
[49] A. Stukowski, Visualization and analysis of atomistic simulation data with OVITO–the Open Visualization Tool, Model. Simulat. Mater. Sci. Eng. 18 (2009), 015012.
[50] É. Maras, et al., Global transition path search for dislocation formation in Ge on Si(001), Comput. Phys. Commun. 205 (2016) 13–21.
[51] L. Wang, et al., In situ atomistic deformation mechanisms of twin-structured nanocrystal Pt, Scripta Mater. 147 (2018) 103–107.
[52] G. Cheng, et al., In situ nano-thermo-mechanical experiment reveals brittle to ductile transition in silicon nanowires, Nano Lett. 19 (2019) 5327–5334.
[53] Z. Liu, et al., Mechanical behavior of InP twinning superlattice nanowires, Nano Lett. 19 (2019) 4490–4497.